# Mechanism and Solvent Catalysis of the Degenerate 1,12-Metalations of [1.1]Ferrocenophanyllithium and [1.1]Ferrocenophanylsodium Studied by NMR Spectroscopy

**Per Ahlberg,* Annika Karlsson, Öjvind Davidsson, Göran Hilmersson, and Martin Löwendahl**

*Contribution from the Department of Organic Chemistry, Göteborg University, S-412 96 Göteborg, Sweden*

*Received June 10, 1996*[⊗]

**Abstract:** Insight into the detailed mechanism of carbon lithiation by an organolithium reagent and of carbon sodiation by an organosodium reagent has been obtained using [1.1]ferrocenophanyllithium (**1**) and [1.1]ferrocenophanylsodium (**3**), respectively. In tetrahydrofuran (THF) **1** and **3** undergo rapid 1,12-proton transfer reactions which are coupled with 1,12-lithium ion and 1,12-sodium ion transfers, respectively. It is concluded that the degenerate rearrangement of **1** does not make use of a pseudorotation mechanism, but occurs by direct conversion of a *syn*-conformer to another *syn*-conformer. Activation parameters ($\Delta H^{\ddagger} = 19$ kJ mol$^{-1}$ and $\Delta S^{\ddagger} = -93$ J K$^{-1}$ mol$^{-1}$) for the degenerate reaction of **1** in THF have been measured by dynamic NMR spectroscopy. The primary isotope effect ($k_H/k_D$) of the 1,12-hydron transfer is 7.4 ± 1.5 at 320 K. The degenerate rearrangement of **1** shows strong solvent dependence, e.g. the reaction is $4 \times 10^3$ times faster in THF than in dimethyltetrahydrofuran (DMTHF). Thus, the rearrangement may be catalyzed by THF in DMTHF. The catalysis is first order in THF at low concentrations of THF. The results show that in the rate-limiting activated complex the lithium ion is coordinating one solvent molecule more than in the initial state. It is paired with a carbanion in which the proton is symmetrically located between the bridge carbons. Compound **3** shows a behavior similar to that of **1**, but it is more fluxtional. It also shows a solvent catalysis that is weaker than for **1**. It is concluded that **3** also exchanges using an activated complex that contains one solvent molecule more than the initial complex.

## 1. Introduction

Much remains to be known about the reaction mechanisms of the enormously useful alkali organometallic reagents.[1] In this paper we present the detailed mechanism of a lithiation and sodiation of carbon. In such reactions, a proton and a metal are transferred between carbons (Scheme 1). The reagents used in the present investigation are [1.1]ferrocenophanyllithium (**1**) prepared from [1.1]ferrocenophane (**2**), Scheme 2, and [1.1]-ferrocenophanylsodium (**3**). Compound **1** has previously been prepared by Mueller-Westerhoff and co-workers.[2] Their studies by NMR spectroscopy indicated that **1** contains a [C−H−C]$^-$ hydrogen bond. This was claimed to be the first verified [C−H−C]$^-$ hydrogen bond.

**Scheme 1**

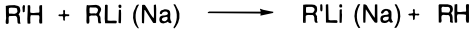


**Scheme 2**

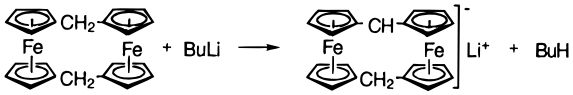


**2** **1**

In preceding papers,[3] we have presented results on the structure of **1** in the solution and in the solid state showing the absence of a [C−H−C]$^-$ hydrogen bond and the importance of ion pairing and solvation. Compound **1** has been found in the solid state as well as in solution to be a monomeric ion pair and to have a *syn*-structure with the lithium ion *exo*-coordinated. In Figure 1 the solid state structure is shown, in which lithium is coordinated to two carbons and two dimethyltetrahydrofuran (DMTHF) molecules.

Compound **1** has been shown by NMR spectroscopy to undergo a fast degenerate lithiation reaction in tetrahydrofuran (THF) which involves an intramolecular 1,12-proton transfer and a 1,12-lithium ion transfer. A proton is moved from C12

* Author to whom correspondence should be sent. Phone: +46 31 7722899. Fax: +46 31 7723840. E-post: Per.Ahlberg@oc.chalmers.se.

⊗ Abstract published in *Advance ACS Abstracts,* February 1, 1997.

(1) (a) Seebach, D. *Angew. Chem., Int. Ed. Engl.* **1988**, *27*, 1624. (b) *Ions and Ion Pairs in Organic Reactions*; Szwarc, M., Ed.; Wiley: New York, 1972; Vols. 1, 2. (c) Bauer, W.; Schleyer, P. v. R. *Adv. Carbanion Chem.* **1992**, *1*, 89. (d) Jackman, L. M.; Bortiatynski, J. *Adv. Carbanion Chem.* **1992**, *1*, 45. (e) Collum, D. B. *Acc. Chem. Res.* **1992**, *25*, 448. (f) Bernstein, M. P.; Collum, D. B. *J. Am. Chem. Soc.* **1993**, *115*, 8008. (g) Kaufmann, E.; Gose, J.; Schleyer, P. v. R. *Organometallics* **1989**, *8*, 2577 and references cited therein. (h) Reich, H. J.; Green, D. P. *J. Am. Chem. Soc.* **1989**, *111*, 8729. (i) Barr D.; Doyle, M. J.; Mulvey, R. E.; Raithby, P. R.; Reed, D.; Snaith, R.; Wright, D. S. *J. Chem. Soc., Chem. Commun.* **1989**, 318. (j) Reich, H. J.; Borst, J. P.; Dykstra, R. R.; Green, D. P. *J. Am. Chem. Soc.***1993**, *115*, 8728 and references cited therein. (k) Fraenkel, G.; Cabral, J. A. *J. Am. Chem. Soc.* **1993**, *115*, 1551. (l) Izatt, R. M.; Bradshaw, J. S.; Nielsen, S. A.; Lamb, J. D.; Christensen, J. J.; Sen, D. *Chem. Rev.* **1985,** *85*, 271. (m) Klumpp, G. W. *Recl. Trav. Chim. Pays-Bas* **1986**, *105*, 1. (n) Gregory, K.; Schleyer, P. v. R.; Snaith, R. *Adv. Inorg. Chem.* **1991**, *37*, 47. (o) Mulvey, R. E. *Chem. Soc. Rev.* **1991**, *20*, 167. (p) Collum, D. B. *Acc. Chem. Res.* **1993**, *26*, 227 (q) Lucht, B. L.; Collum, D. B. *J. Am. Chem. Soc.* **1994**, *116*, 6009.

(2) (a) Mueller-Westerhoff, U. T.; Nazzal, A.; Prössdorf, W. *J. Am. Chem. Soc.* **1981**, *103*, 7678 and references cited therein. (b) Dagani, R. *Chem. Eng. News* **1982**, 23. (c) Mueller-Westerhoff, U. T. *Angew. Chem., Int. Ed. Engl.* **1986**, *25*, 702.

(3) (a) Ahlberg, P.; Davidsson, Ö. *J. Chem. Soc., Chem. Commun.* **1987**, 623. (b) Ahlberg, P.; Davidsson, Ö.; Johnsson, B.; Mc Ewen, I.; Rönnqvist, M. *Bull. Soc. Chim. Fr.* **1988**, 177. (c) Davidsson, Ö.; Löwendahl, J-M.; Ahlberg, P. *J. Chem. Soc., Chem. Commun.* **1992**, 1004. (d) Ahlberg, P.; Davidsson, Ö.; Hilmersson, G.; Löwendahl, M.; Håkansson, M. *J. Chem. Soc., Chem. Commun.* **1994**, *1573.* (e) Ahlberg, P.; Davidsson, Ö.; Löwendahl, M.; Hilmersson, G.; Karlsson, A.; Håkansson, M. *J. Am. Chem. Soc.* **1997**, *119*, 1745.

S0002-7863(96)04346-6 CCC: $14.00 

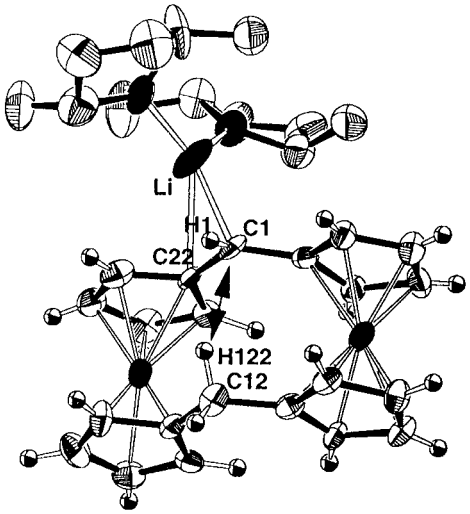


**Figure 1.** A drawing of the solid state structure of **1**, crystallized from DMTHF.

**Scheme 3**

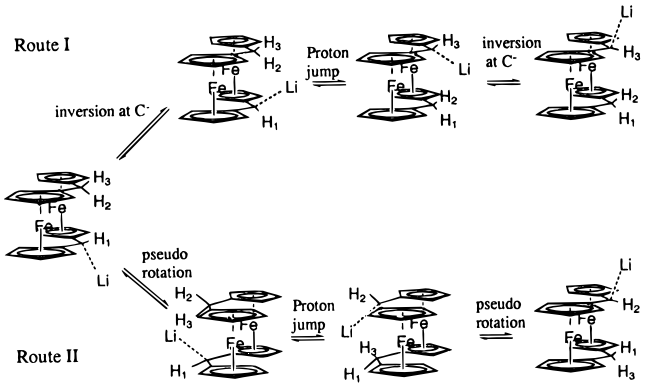


to C1 and this transfer is accompanied by the motion of $Li^+$ from an *exo*-position at C1 to another *exo*-position at the former C12.

In this paper we report results on the detailed mechanism and solvent catalysis of the degenerate rearrangement of **1** along with studies of the solvent catalysis of the degenerate rearrangement of **3**.

## Results and Discussion

Two possible routes for the degenerate lithiation are shown in Scheme 3. As indicated by the hydrogen labels, different protons are transferred by the two routes. Route I makes use of *syn*-structures, which directly undergo the degenerate lithiation reaction by 1,12-*endo*-proton transfer and migration of $Li^+$ from an *exo*-position via two *endo*-positions to another *exo*-position. Route II, on the other hand, makes use of a pseudorotation[4] to relocate $Li^+$ from its initial *exo*-position to an *endo*-position. Then the 1,12-proton transfer takes place in which a proton that initially was an *exo*-proton is being transferred. After the transfer, another pseudorotation takes the $Li^+$ from an *endo*-position to an *exo*-position and moves the transferred proton to an *exo*-position.

To differentiate these two routes, lithiated $\beta$-ethyl[1.1]-ferrocenophane (**4**) was prepared from $\beta$-ethyl[1.1]ferrocenophane.[5] $^1$H NMR spectroscopy (Figure 2) showed that ethyl-substituted **1** is present as two isomer pairs **5a**, **5b** and

(4) Löwendahl, M.; Davidsson, Ö.; Ahlberg, P. *J. Chem. Res. Synop,* **1993**, 40.

(5) Karlsson, A.; Löwendahl, M.; Hilmersson, G; Davidsson, Ö.; Ahlberg, P. *J. Phys. Org. Chem.* **1996**, 9, 436.

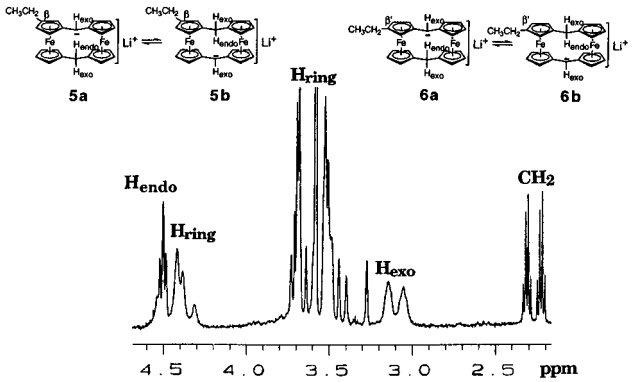


**Figure 2.** $^1$H NMR spectrum (obtained at 499.92 MHz) of **5** and **6** in THF-$d_8$ at +21°C.

**Scheme 4**

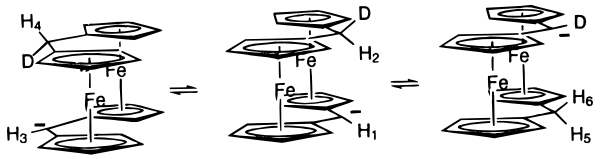

**6a**, **6b**. The isomers in each pair are interconverting by fast degenerate rearrangements, as shown in Figure 2. There is obviously no fast interconversion of the two isomer pairs at 21 °C in THF.

Lowering the temperature resulted in band broadening and splitting of the signals of each isomer like in the parent carbanion **1**. A $^1$H,$^1$H NOESY experiment showed no crosspeaks for the signals in **5** and **6**, giving no indication that **5** and **6** are interconverting. The results of these experiments and the investigation of **1** using buildup transient NOEs show that the proton being transferred is the *endo*-methylene proton in a *syn*-structure. For the transient NOE experiments a solution of the bridge monodeuteriated compound **7** was used in DEE-$d_{10}$. In this solvent the intramolecular 1,12-lithiation is slow on the NMR time scale. The $^1$H NMR spectrum of the bridge protons showed, besides the singlet from the proton bonded to the carbanionic carbon at $\delta$ 2.70, a doublet (H in $CH_2$) and a singlet (H in CHD) at $\delta$ 3.61−3.67 and another doublet (H in $CH_2$) and singlet (H in CHD) at $\delta$ 4.50−4.56. In Scheme 4 the three different isotopomers with *syn*-structures are shown together with their interconversions.

The signals from the protons at the carbanionic carbons ($H_1$ and $H_3$) in two of the isotopomers irradiated with a 180° pulse and the initial buildup rates of the transient NOEs of the other bridge proton signals with time were studied. At short mixing times (∼0.5 s), the signals from the protons at $\delta$ 4.50−4.56 showed positive NOEs and those at $\delta$ 3.62−3.67 negative NOEs.

These results clearly show that in one of the isotopomers present in solution the $HC^-$ proton is close in space to the proton in the CHD group, since a positive NOE is observed. This is not consistent with an *anti*-isomer. It was concluded in the preceding paper[3e] that **1** has a *syn*-structure and that in the isotopomer the CHD proton is in *endo*-position, and as a consequence the $Li^+$ must be in an *exo*-position in **1**.

The hydrogen $H_2$ becomes $H_6$ upon rearrangement, and $H_6$ therefore also shows a positive NOE.

The signals at $\delta$ 3.62−3.67 are concluded to be due to $H_4$ and $H_5$. $H_5$ exhibits a negative NOE because the lithiation converts $H_1$ into $H_5$. $H_4$, which is at a long distance from $H_3$, also experiences a negative NOE because of exchange through the rearrangement shown in Scheme 4. These results are

**Scheme 5**

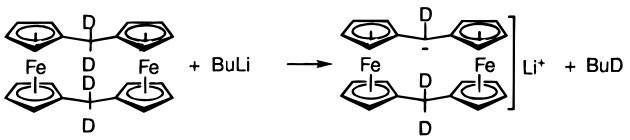


**8** **9**

**Scheme 6**

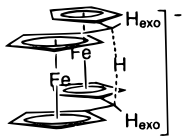


consistent with direct transfer of an *endo*-proton in **1** from C12 in a *syn*-structure to C1 to yield an identical *syn*-structure with the transferred proton in *endo*-position.

Thus, the major degenerate rearrangement route used by **1** is route I in Scheme 3, which does not involve any pseudorotation. Pseudorotation is fast in **2**[4]—the precursor of **1**—but obviously much slower in **1**, making contribution of such a mechanism unimportant for the degenerate lithiation.

**Rate-Limiting Step.** The degenerate rearrangement of **1** could have several rate limiting steps. Kinetic deuterium isotope effects are of course the natural tool to probe whether the proton transfer is rate limiting.[6] Tetradeuterated ferrocenophane (**8**) was synthesized by repeated ionization of ferrocenophane with BuLi and quenching with $D_2O$. Trideuterated carbanion (**9**) was prepared in the usual way (Scheme 5), and the rate constant ($k_D$) for the degenerate rearrangement was measured by DNMR. The isotope effect obtained was $k_H/k_D = 7.4 \pm 1.5$ (320 K). Thus, the proton is being transferred in the rate-limiting step. The magnitude of the isotope effect suggests that in the transition state (Scheme 6) of this step the proton is symmetrically located between the bridge carbons.[6]

The isotope effect at 185 K is $16.4 \pm 3.3$. Assuming the isotope effect is semiclassical, one could explain the observed temperature dependence without involving tunneling.[6]

To find out whether the rate-limiting proton transfer takes place in a free carbanion, a carbanion/lithium ion pair or an aggregate, e.g. a dimer of ion pairs, the dependence of $k_{obs}$ on reagent concentration was investigated. Dilution (ca. 7-fold) of THF and DMTHF solutions of **1** at +25 °C with THF or DMTHF did not significantly change (±15%) the observed rate constants respectively for the degenerate rearrangement. Since we have previously shown that **1** is monomeric in DMTHF, it is concluded that **1** is not aggregated in the rate-limiting activated complex.

Compared with DEE and DMTHF, THF has been found to favor small organolithium aggregates, and therefore aggregation of **1** is not important in its degenerate rearrangement.

The concentration independence of the observed rate constant also shows that the transfer does not take place in a free carbanion but in a carbanion paired with a solvated lithium cation. Thus, our results above indicate solvent association in the transition state and that $k_{obs}$ will be solvent dependent.

**Solvent Effects and Catalysis of the Lithiation Reaction.** Studies of the temperature dependence of the degenerate rearrangement of **1** revealed some surprising results. Using the $^1$H NMR spectral data shown in Figure 1 in the preceding paper,

(6) Melander, L.; Saunders, W., In *Reaction Rates of Isotopic Molecules*, 2nd ed.; John Wiley & Sons, Inc.: New York, 1979.

(7) (a)Lucht, B. L.; Collum, D. B. *J. Am. Chem. Soc.* **1995**, *117*, 9863. (b) Hilmersson, G. Davidsson, Ö. *J. Org. Chem.* **1995**, *60*, 7660.

**Table 1.** Influence of Solvent and Temperature upon the Degenerate Proton Transfer in **1**

| temp/°C | solvent | $k_{obs}/s^{-1}$ |
|---|---|---|
| 21 | THF | $3.2 \times 10^4$ |
| 21 | MTHF[a] | $9.4 \times 10^3$ |
| 21 | DMTHF | 10 |
| 21 | DEE | 8.3 |
| −100 | THF | 63 |

[a] MTHF = 2-methyltetrahydrofuran.

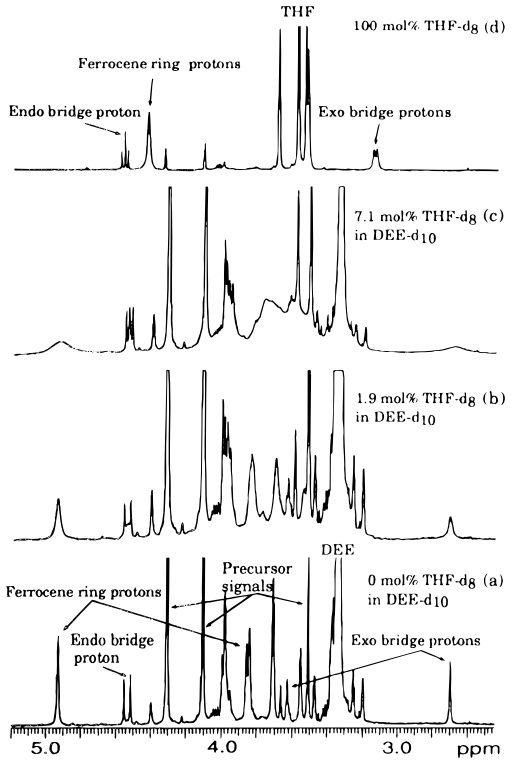


**Figure 3.** $^1$H NMR spectra (obtained at 499.92 MHz) of 4 mM solutions of **1** at 27.0 ± 0.5 °C in different mixtures of DEE-$d_{10}$/THF-$d_8$: (a) in pure DEE-$d_{10}$; (b) in DEE-$d_{10}$ containing 1.9 mol % THF-$d_8$; (c) in DEE-$d_{10}$ containing 7.1 mol % THF-$d_8$; and (d) in pure THF-$d_8$.

the activation parameters were determined. Instead of an activation entropy being close to zero, a considerable negative entropy ($\Delta S^{\ddagger}$) was measured, i.e. −93 J K$^{-1}$ mol$^{-1}$. The enthalpy of activation was only 19 kJ mol$^{-1}$. These results and the results of the dilution experiments above therefore suggest that the solvent plays a key role in the mechanism of the degenerate rearrangement.

Indeed the rate of the degenerate process showed strong solvent dependence (Table 1). The ratio of the rate constants in THF ($k_{THF}$) and DEE ($k_{DEE}$) is approximately 4000 at room temperature. The large ratio suggests that the reaction in DEE is retarded relative to that in THF due to larger sterical requirements of DEE which lead to larger steric repulsions in the activated complex in which $Li^+$ is coordinating more solvent molecules than in the initial complex.

Some experiments described below reveal details of solvation in the rate-limiting step of the degenerate rearrangement.

In DEE at 27.0 ± 0.5 °C the intramolecular proton transfer in **1** is slow (cf. Figure 3), and three different $^1$H NMR signals are obtained for the bridge protons. The singlet at $\delta$ 2.70 originates from the proton on the carbanionic bridge carbon. The doublet at $\delta$ 3.65 ($J$ = 19.2 Hz) is due to the *exo*-proton of the bridge methylene group and the doublet at $\delta$ 4.54, $J$ = 19.2 Hz) has been assigned to the *endo*-proton. The spectrum in

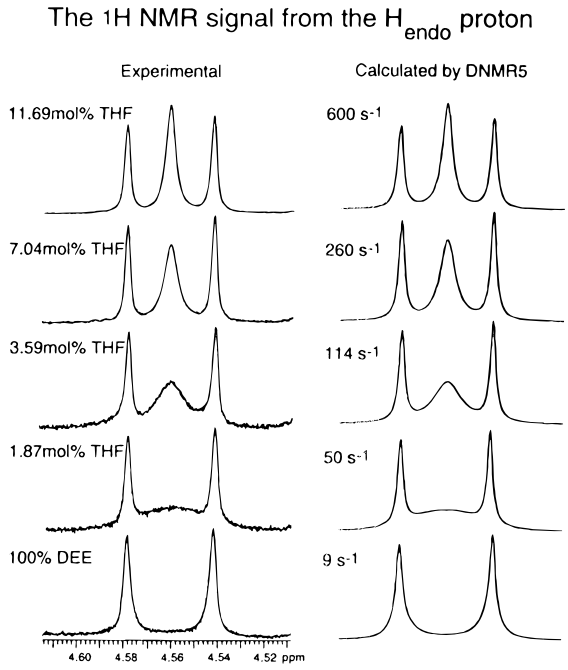


**Figure 4.** Partial $^1$H NMR spectra (obtained at 499.92 MHz) of 4 mM solutions of **1** at 27.0 ± 0.5 °C in different mixtures of DEE-$d_{10}$/THF-$d_8$ and the corresponding calculated spectra using DNMR5.

Figure 3a was obtained with ca. 4 mM solution of **1**, crystallized from DMTHF, in DEE-$d_{10}$. Addition of small amounts of THF-$d_8$ (1.9 mol % of the solvent) resulted in a dramatic increase of the intramolecular proton transfer rate (Figure 3a), as indicated by broadening of the singlet at $\delta$ 2.70 and the broad singlet at $\delta$ 3.65, resulting from the collapse of the doublet at the same chemical shift.

Addition of more THF-$d_8$ increased the broadening of the two singlets (Figure 3c). In pure THF-$d_8$ (Figure 3d) there is a fast exchange of the *exo*-methylene proton with the proton bonded to the carbanionic bridge carbon, as indicated by the doublet at $\delta$ 3.14 ($J$ = 9.6 Hz) and the *endo*-methylene triplet at $\delta$ 4.56 ($J$ = 9.6 Hz).

The rate constant ($k_{obs}$) for the degenerate rearrangement at different mol % THF-$d_8$ was obtained from the band shape of the singlet at $\delta$ 2.70 and the complex *endo*-proton signal at $\delta$ 4.56 using simulations by the DNMR5 program.[8] Fits to the former signal gave the more accurate rate constants. The simulated and experimentally obtained spectra are shown in Figure 4.

In Figure 5 the observed rate constants have been plotted vs mol % THF-$d_8$ of the solvent. There is an approximately linear dependence on mol % THF up to about 2 mol % THF-$d_8$. At higher THF-$d_8$ concentrations $k_{obs}$ increases faster. Obviously, the 1,12-lithiation is catalyzed by THF. At about 2 mol % THF-$d_8$ 85% of the activated complexes are catalysis complexes. At 10 mol % THF-$d_8$ about 99% of the rearrangement emanates from catalysis.

**Mechanism.** The nearly linear dependence at low mol % THF-$d_8$ shows that the proton transfer is first order in THF in the concentration interval. It is concluded that the new THF-catalyzed route that has been opened makes use of rate-limiting activated complexes containing one THF molecule more than the initial state complex.

The measured $\Delta S^{\ddagger} = -93$ J K$^{-1}$ mol$^{-1}$ shows that only one solvent molecule is immobilized on going to the transition state. The low $\Delta H^{\ddagger} = 19$ kJ mol$^{-1}$ is explained by a combination of

(8) Stephenson, D. S.; Binsch, G. *QCPE* **1978**, *365*, 11.

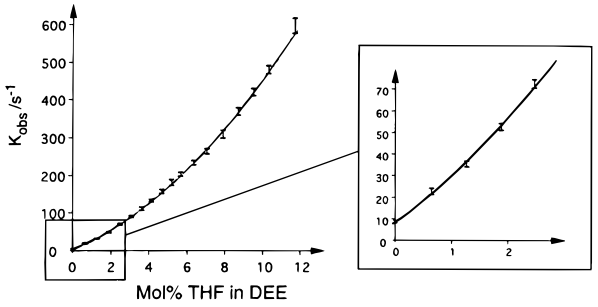


**Figure 5.** The observed rate constant $k_{obs}$ at 27.0 ± 0.5 °C for the degenerate rearrangement plotted against mol % THF-$d_8$ in DEE-$d_{10}$. The plot shows first-order dependence in THF-$d_8$ at mol % THF <2. At higher mol % THF the reaction order in THF is larger than 1. The size of the I markers indicate estimated maximal errors due to errors in $k_{obs}$, THF concentration, and temperature. The curve has been obtained from simulations using eq 3 derived below.

**Scheme 7**

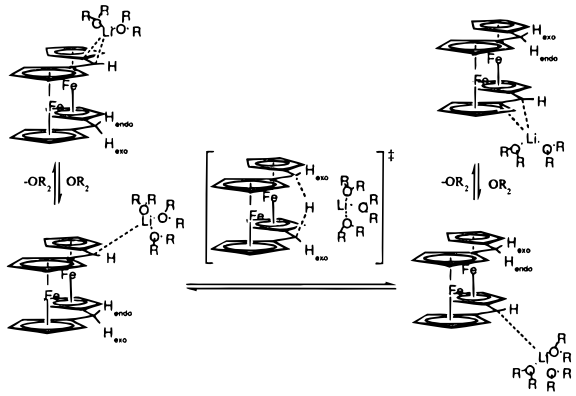

the negative enthalpy caused by increased ligation of $Li^+$ and positive activation enthalpy contributions. Thus, the $\Delta G^{\ddagger}_{300K}$ = 47 kJ mol$^{-1}$ is dominated by the $T\Delta S^{\ddagger}$ term. All results taken together are consistent with the mechanism shown in Scheme 7.

It is assumed that intermediates in which $Li^+$ is coordinated to the carbanion and three ethereal ligands are first formed. The increased coordination of $Li^+$ results in increased ether dipole−anion and ether dipole−ether dipole repulsions, weakening the attraction of $Li^+$ and the carbanionic ligand. $Li^+$ and the carbanion are therefore more separated in the intermediate. This prepares the system for a low barrier proton transfer. The proton is transferred intramolecularly, but it is not possible to tell if the lithium ion transfer is also intramolecular because of fast lithium exchange reactions. In the rate-limiting activated complex, the hydron is half transferred between the carbons. The carbanionic charge is in part localized to the carbons in between which the proton is being transferred. The [C−H−C]$^-$ part of the activated complex is reminiscent of a strong hydrogen bond (which has been shown to be absent in the initial state complex). The transition state acquires stabilization by pairing the carbanion with a lithium ion coordinated to three ethereal ligands. The intermediate obtained by the rearrangement then expels a solvent molecule, yielding an initial state complex and thus completing the degenerate alkalimetalation.

The curve that simulates the experimental results in Figure 5 has been obtained using an equation derived from the mechanistic model described below.

In pure DEE, **1** is solvated by two DEE molecules in the initial state. In mixtures of DEE and THF, **1** could also be solvated by one DEE molecule and one THF molecule or by two THF molecules. The three initial state complexes which

**Scheme 8**

$$FLi(DEE)_2 + THF \overset{K_1}{\rightleftharpoons} FLi(DEE)(THF) + DEE$$

$$FLi(DEE)(THF) + THF \overset{K_2}{\rightleftharpoons} FLi(THF)_2 + DEE$$

**Scheme 9**

$$1 \underset{k_{obs}}{\overset{k_{obs}}{\rightleftharpoons}} 1$$

are assumed to be in fast equilibrium are named $FLi(DEE)_2$, FLi(DEE)(THF), and $FLi(THF)_2$, respectively. The equilibria are shown in Scheme 8. The corresponding suggested transition states containing one solvent molecule more than an initial complex are $FLi(DEE)^{\ddagger}_3$, $FLi(DEE)_2(THF)^{\ddagger}$, $FLi(DEE)(THF)^{\ddagger}_2$, and $FLi(THF)^{\ddagger}_3$.

By the degenerate lithiation reaction solvated FLi is converted into itself by an observed first-order rate constant $k_{obs}$, which is defined in Scheme 9. The rate in the forward direction is $k_{obs}$ [**1**] where [**1**] = [$FLi(DEE)_2$] + [FLi(DEE)(THF)] + [$FLi(THF)_2$]. Using the equilibrium constants $K_1$ and $K_2$ defined in Scheme 7, the following expression for [**1**] is derived.

$$[\mathbf{1}] = [FLi(DEE)_2]\left(1 + K_1\frac{[THF]}{[DEE]} + K_1K_2\frac{[THF]^2}{[DEE]^2}\right) \quad (1)$$

The rate $k_{obs}$ [**1**] could be expressed as the sum of the rates through the four different types of activated complex using $FLi(DEE)_2$ as a common reference initial state as shown in eq 2.

$$k_{obs}[\mathbf{1}] = k_1[FLi(DEE)_2][DEE] + k_2[FLi(DEE)_2][THF] + k_3[FLi(DEE)_2]\frac{[THF]^2}{[DEE]} + k_4[FLi(DEE)_2]\frac{[THF]^3}{[DEE]^2} \quad (2)$$

A combination of eqs 1 and 2 gives the following, eq 3, in which $k_{obs}$ is expressed as a function of the solvent concentrations [DEE] and [THF], the rate constants $k_1$, $k_2$, $k_3$, and $k_4$ together with the equilibrium constants $K_1$ and $K_2$.

$$k_{obs} = \frac{k_1[DEE]^3 + k_2[DEE]^2[THF] + k_3[THF]^2[DEE] + k_4[THF]^3}{[DEE]^2 + K_1[DEE][THF] + K_1K_2[THF]^2} \quad (3)$$

The rate constants $k_1$ and $k_4$ were calculated from measured $k_{obs}$ in pure DEE and pure THF, respectively. At low THF concentrations (<1 mol % THF), the dependence of $k_{obs}$ on [THF] is nearly linear ($k_{obs} = k_1[DEE] + k_2[THF]$), and therefore $k_2$ has been determined independently of $k_3$, $K_1$, and $K_2$. The latter three parameters were determined from a simulation of the curve shown in Figure 5 using eq 3. Since the THF concentration interval used in the present study is rather narrow (~12 mol %), the latter parameters determined in the simulation are less accurate.

The optimal parameters obtained are $k_1 = 0.9\ M^{-1}\ s^{-1}$; $k_2 = 2.0 \times 10^2\ M^{-1}\ s^{-1}$; $k_3 = 2.5 \times 10^3\ M^{-1}\ s^{-1}$; $k_4 \sim 2.7 \times 10^3\ M^{-1}\ s^{-1}$; $K_1 \sim 1.0$ and $K_2 \sim 1.0$. The qualitative standard free energy diagram shown in Figure 6 is based on these data.

At a first glance the values of the obtained parameters are surprising. In particular the fact that $K_1$ and $K_2$ are of about equal magnitude and being ~1. The explanation is that, for example, $FLi(DEE)_2$ is not sterically crowded, and therefore replacement of one DEE for one THF molecule does not change the steric interactions significantly. As a consequence $K_1 \sim 1$. Similarly, the steric interactions in FLi(DEE)(THF) and $FLi(THF)_2$ are concluded to be similar. Thus, $K_2$ is also close to unity. At the lowest [THF-$d_8$] (~0.6 mol % of the solvent) used in the experiments (Figure 5), the [THF-$d_8$] is about 20 times larger than [**1**]. If $K_1$ and $K_2$ both are ~1, the fraction of initial state complexes only solvated by DEE-$d_{10}$ is ~ 100% at low mol % THF-$d_8$.

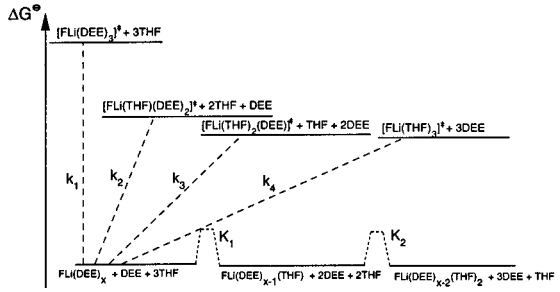


**Figure 6.** Standard free energy diagram showing the four transition states and the three different initial states for the solvent-catalyzed degenerate lithiation reaction in **1**.

The second-order rate constants $k_1$, $k_2$, $k_3$, and $k_4$ correspond to activated complexes containing three DEE molecules, two DEE molecules and one THF molecule, one DEE molecule and two THF molecules, and three THF molecules ligated to Li in the ion pairs, respectively. The common reference initial state is $FLi(DEE)_3$ + 3THF for $k_1$ to $k_4$.

The fact that $k_2$ is about 220 times larger than $k_1$ expresses the different steric requirements of DEE and THF in the activated complexes. The steric repulsions in the $k_3$-activated complex would be even smaller than that in the $k_2$ complex. Indeed, $k_3$ is only 13 times larger than $k_2$. Apparently replacement of a second DEE molecule by a THF yields a smaller stabilization of the transition state than replacement by the first one, because the $k_2$ complex is less crowded than the $k_1$ complex. Accordingly replacement of the third DEE by a THF molecule results only in a slightly increased stabilization, i.e. $k_3 \cong k_4$. The relative contribution of the different activated complexes to the catalysis vary strongly with the [THF].

Below two other related mechanisms are considered which yield practically the same $k_{obs}$ dependence on [THF] as eq 3 which was derived assuming disolvated initial complexes and trisolvated activated complexes. Assumption of disolvated initial complexes and tetrasolvated activated complexes leads to eq 4.

$$k_{obs} = \frac{k'_1[DEE]^4 + k'_2[DEE]^3[THF] + k'_3[THF]^2[DEE]^2 + k'_4[DEE][THF]^3 + k'_5[THF]^4}{[DEE]^2 + K_1[DEE][THF] + K_1K_2[THF]^2} \quad (4)$$

Since the rate constants in eq 4 are different than those in eq 3, these are primed. In view of the narrow concentration interval of THF used in the measurements, $k_{obs}$ in eq 4 shows within experimental errors the same dependence on [THF] as does eq 3.

However, since in the eq 4 mechanism two solvent molecules are immobilized in the transition state compared with one in the eq 3 mechanism, a standard activation entropy about two times larger than measured is expected for this mechanism. This indicates that the eq 4 mechanism is not of significance in our system.

In the second related mechanism it is assumed that the initial state complexes are trisolvated, i.e. they contain one solvent molecule more than in the solid state structure of **1**, and that

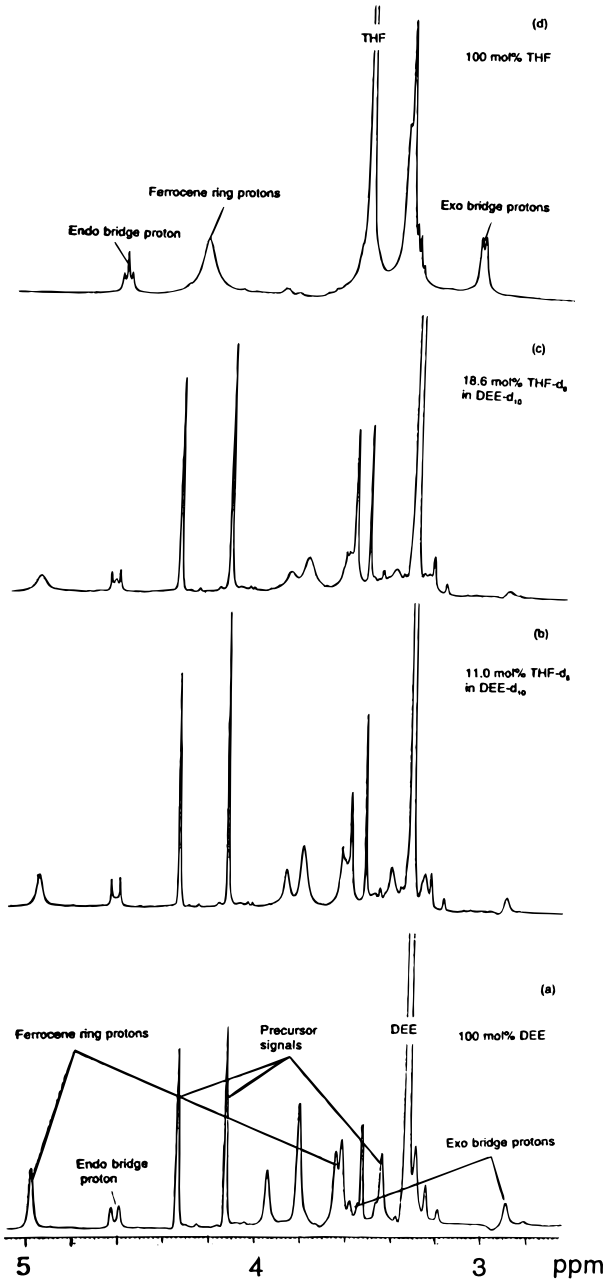


**Figure 7.** $^1$H NMR spectra (obtained at 499.92 MHz) of 9 mM solutions of **3** at $-44 \pm 0.5$ °C in different mixtures of DEE-$d_{10}$/THF-$d_8$: (a) in pure DEE-$d_{10}$; (b) in DEE-$d_{10}$ containing 11.0 mol % THF-$d_8$; (c) in DEE-$d_{10}$ containing 18.6 mol % THF-$d_8$; and (d) in pure THF-$d_8$.

the activated complexes are tetrasolvated. This assumption yields eq 5.

$$k_{obs} = \frac{k''_1[DEE]^4 + k''_2[DEE]^3[THF] + k''_3[THF]^2[DEE]^2 + k''_4[DEE][THF]^3 + k''_5[THF]^4}{[DEE]^3 + K''_1[DEE]^2[THF] + K''_1K''_2[DEE][THF]^2 + K''_1K''_2K''_3[THF]^3} \quad (5)$$

Since the rate constants and equilibrium constants are different from those in eqs 3 and 4 they have been double primed. Equation 5 like eq 4 gives a $k_{obs}$ dependence on [THF] which is practically identical with that exhibited by eq 3. Interestingly the eq 5 mechanism is expected to show about the same standard activation entropy as the eq 3 mechanism. Thus our experimental results are consistent also with the eq 5 mechanism.

**Solvent Catalysis of the 1,12-Sodiation in 3.** To get further insight into the role of the alkali cation and solvent in alkalimetalations, [1.1]ferrocenophanylsodium (**3**) was prepared from **2** and $CH_3Na$ in DEE-$d_{10}$. The degenerate rearrangement of **3** has been studied by NMR spectroscopy.

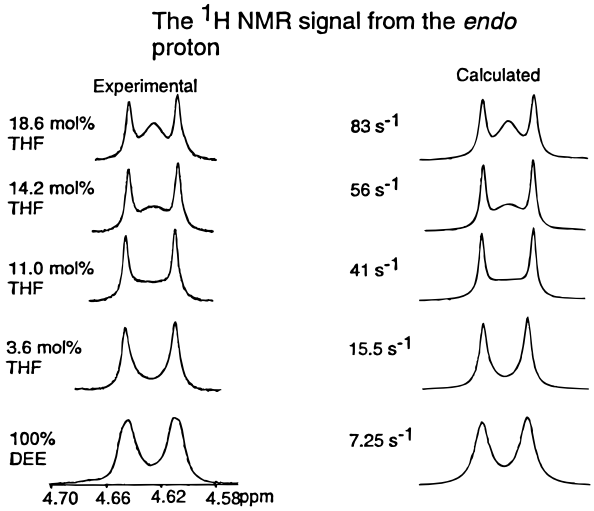


**Figure 8.** Partial $^1$H NMR spectra (obtained at 499.92 MHz) of 9 mM solutions of **3** at $-44 \pm 0.5$ °C in different mixtures of DEE-$d_{10}$/THF-$d_8$ and the corresponding calculated spectra using DNMR5.

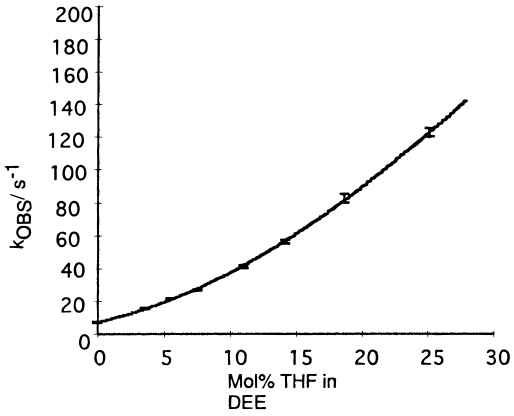


**Figure 9.** The observed rate constant $k_{obs}$ at $-44 \pm 0.5$ °C for the degenerate rearrangement of **3** plotted against mol % THF-$d_8$ in DEE-$d_{10}$. The plot shows first-order dependence in THF-$d_8$ at mol % THF <8. At higher mol % THF the reaction order in THF is larger than 1. The size of the I markers indicate estimated maximal errors due to errors in $k_{obs}$, THF concentration, and temperature. The curve has been obtained from simulations using eq 3.

Compound **3** is found to be much more reactive than **1**. The observed rate constant for the degenerate rearrangement of **3** at $-44$ °C has about the same value as $k_{obs}$ for **1** at $+27$ °C DEE-$d_{10}$.

The sodium ion is bigger ($r_{Na} = 0.95$ Å) than the lithium ion ($r_{Li} = 0.60$ Å). Therefore, the attraction of the $Na^+$ to the ferrocenophanyl anion in **3** is weaker than the corresponding interaction involving $Li^+$ in **1**. The corresponding attraction difference in the activated complexes is expected to be smaller. This explains why **3** is more reactive than **1**.

Interestingly, the 1,12-sodiation of **3** in DEE-$d_{10}$ is also found to be catalyzed by THF-$d_8$, but the catalysis is weaker than for **1**; see Figure 7.

In Figure 7 the $^1$H NMR spectra of **3** in DEE-$d_{10}$ with different amounts of THF-$d_8$ added is shown. The rate constant for the degenerate rearrangement at different mol % THF-$d_8$ was obtained from band shape analysis of the triplet from the *endo* bridge proton at $\delta$ 4.56 (Figure 8). A plot of $k_{obs}$ vs mol % THF in the solvent is displayed in Figure 9. The simulated

curve has been obtained using an equation having the same $k_{obs}$ dependence on [THF] as eq 3.

The number ($x$) of DEE molecules that solvates $Na^+$ in the reference initial state $FLi(DEE)_x$ is not known. However, since the sodium ion is bigger than the lithium ion, there is space for coordination of more ligands but the surface charge is smaller for $Na^+$. A likely number of ethereal molecules coordinating **3** in the initial state might therefore be similar to that for **1**. The transition states corresponding to $k_1$, $k_2$, $k_3$, and $k_4$ are $FNa(DEE)^{\ddagger}_{x+1}$, $FNa(DEE)_x(THF)^{\ddagger}$, $FNa(DEE)_{x-1}(THF)^{\ddagger}_2$ and $FNa(DEE)_{x-2}(THF)^{\ddagger}_3$, respectively.

As seen in Figure 9, the curve fits excellently to the observed rate constants. It is concluded that **3** like **1** in the rate-limiting rearrangement activated complexes may contain only one ethereal ligand more than in the initial state complex. Assuming that **3** contains two solvent ligands in the initial complexes and three solvent ligands in the activated complexes, the following parameters were obtained at −44 °C: $k_1 = 0.75\ M^{-1}\ s^{-1}$; $k_2 = 2.0 \times 10\ M^{-1}\ s^{-1}$; $k_3 \sim 1.0 \times 10^2\ M^{-1}\ s^{-1}$; $k_4 \sim 1 \times 10^2\ M^{-1}\ s^{-1}$; $K_1 \sim 1$; and $K_2 \sim 1$. The inaccuracy of $k_3$, $k_4$, $K_1$, and $K_2$ is large. A standard free energy diagram qualitatively similar to that in Figure 6 may be constructed on the basis of these parameters.

The similarity of $K_1$ to $K_2$ and the fact that the values of both are close to unity may be explained as for **1**. The relative values of $k_1$ to $k_4$, which express weaker catalysis than with **1**, is explained as for **1**, assuming smaller steric interaction differences.

## Experimental Section

In the preceding publication,[3e] general procedures for purification and handling of solvents and chemicals as well as preparation of precursors except for [11,12-$^2H_4$][1.1]ferrocenophane[3b] and their lithium salts have been reported together with NMR spectroscopy including transient 1D NOE experiments.

**Preparation of [1.1]Ferrocenophanylsodium (3).** Procedures similar to those used for the preparation of **1** were employed. Compound **3** was made directly in an NMR tube. [1.1]Ferrocenophane (**2**) (2.8 mg, 7.1 μmol) was dissolved in 0.6 mL of DEE-$d_{10}$, the solution was cooled to −70 °C, and 20 μL of a 0.21 M slurry of $CH_3Na$ in hexane (4.2 μmol) was added. The fraction of **3** formed was monitored by $^1H$ NMR at −44 °C. Successive additions of $CH_3Na$ gave solutions with wanted composition. In between each addition the reaction mixture was allowed to reach room temperature.

The preparation of $CH_3Na$ presented below is similar to that for $CH_3K$[9] and *n*-BuNa.[10] Sodium *tert*-butoxide (0.62 g, 7.2 mmol) was dissolved in 5 mL of DEE, and the obtained solution was cooled in acetone/ice. Using a syringe, 4.7 mL of a 1.6 M solution of $CH_3Li$ (7.5 mmol) in DEE was added, and the mixture was stirred for 5 min while solid material was formed. After centrifugation the supernatant liquid was removed. The remaining solid material was washed twice with 2 × 10 mL of DEE and flushed with argon overnight. A slurry was made with hexane, and this was used in the above experiments. In the catalysis experiments [**2**] < [**3**] and the concentration of [**3**] in DEE-$d_{10}$ was about 9 mM.

**Solvent Catalysis.** Typically 15 mg of [1.1]ferrocenophane was transferred to an NMR tube (cf. carbanion preparation).[3e] The tube was removed from the glovebox, and 250 μL of DMTHF was added. Then 100 μL of 1.6 M BuLi in hexane was added, and the tube was stored in a plastic bag filled with argon in the freezer overnight. The next day, crystals, which are dark red needles, usually had formed and the tube was brought into the glovebox. Most of the solvent was removed, and the crystals were washed twice with heptane. The tube was removed from the glovebox and attached to the vacuum line in order to remove the last traces of solvent. Usually 800 μL of DEE-$d_{10}$ was added, and a $^1H$ NMR spectrum was recorded. Mixtures of DEE-$d_{10}$ and THF-$d_8$ were prepared and used for additions of small amounts of THF-$d_8$. NMR spectra were recorded after each addition. Rate constants ($k_{obs}$) were determined from band shape analysis using DNMR5. The same procedure was used for titrations in other solvents. Reproducibility was demonstrated using two different samples, prepared from crystals obtained from two different crystallizations that were investigated in parallel.

Compound **3** was not recrystallized before use in the catalysis experiments. The prepared solutions of **3** were used directly, and the procedure was similar to that for **1**.

**Acknowledgment.** We are grateful to Docent Lars Baltzer and Professor Gideon Fraenkel for stimulating discussions and advice and to Docent Baltzer for assistance in some of the NMR experiments. We also thank the Swedish Natural Science Research Council for support.

JA964346E

(9) Weiss, E.; Sauerman, G. *Chem. Ber*. **1970**, *103*, 265.
(10) Schade, C.; Bauer, W.; Schleyer, P. v. R. *J. Organomet. Chem*. **1985**, *C25*, 295.